Original Paper

Cellular Physiology and Biochemistry

Cell Physiol Biochem 2008;21:385-394

Accepted: January 03, 2008

Characterization and Comparison of Na^+, K^+ and Ca^{2+} Currents Between Myocytes from Human Atrial Right Appendage and Atrial Septum

Dongmei Gong[a,d], Yong Zhang[a], Benzhi Cai[a], Qingxin Meng[b], Shulin Jiang[b], Xia Li[c], Luchen Shan[a], Yanyan Liu[a], Guofen Qiao[a], Yanjie Lu[a,d] and Baofeng Yang[a,d]

[a]Department of Pharmacology; [b]Department of Cardiac Surgery, the 2nd Affiliated Hospital; [c]Department of Bioinformatics, and [d]State-Province Key Laboratories of Biomedicine Pharmaceutics, Harbin Medical University, Harbin

Key Words

Action potential • Ion channels • Electrophysiology • Regional heterogeneity • Human atrium

Abstract

Atrial pacing to reduce paroxysmal atrial fibrillation recurrences is performed in right atrial appendage (RAA) traditionally. However, recent studies indicate that atrial septal (AS) pacing produces better outcomes than the RAA pacing. The underlying mechanisms for this difference remained unclear. One possible explanation for the superiority of AS pacing over RAA pacing is that the two different regions have distinct electrophysiological properties. The study was to explore whether there indeed exist regional differences of electrical activities between RAA and AS, using whole-cell patch clamp techniques. The results showed that RAA cells had longer action potential duration, more negative resting potential and greater amplitude of action potential, whereas AS cells had more rapid depolarizing velocity. The sodium current was significantly smaller in RAA cells, whereas the calcium current was markedly smaller in AS cells. The transient outward K^+ current was similar in both regions. The ultrarapid delayed rectifier K^+ current was greater in RAA than that in AS cells. The inward rectifier K^+ current was similar at potentials more negative to -60 mV in both regions. The results indicate that RAA and AS of patients with rheumatic heart disease possess distinct electrophysiological properties. These differences provided a rational explanation for the different efficacies in treating atrial fibrillation by atrial pacing in RAA and AS regions.

Introduction

Atrial fibrillation (AF) is the most common cardiac arrhythmia in clinical practice and can lead to potentially serious clinical consequences, including thromboembolism,

KARGER

Fax +41 61 306 12 34
E-Mail karger@karger.ch
www.karger.com

1015-8987/08/0216-0385$24.50/0

Accessible online at:
www.karger.com/cpb

Baofeng Yang
Department of Pharmacology, Harbin Medical University
Baojian Road 157, Harbin, Heilongjiang 150081 (P. R. China)
Tel. +86 451 86671354, Fax +86 451 86675769
E-Mail yangbf@ems.hrbmu.edu.cn

impaired physical capacity, reduced left ventricular function, and stroke [1]. The treatment of AF remains suboptimal because of limited efficacy and potential side effects of drug therapy [2]. A variety of non-pharmacological approaches have been used in the management of AF, including pacemakers, implantable atrial defibrillators, catheter ablation, and surgery. A newer strategy is to use atrial pacing to reduce paroxysmal AF recurrences and consequent progression to chronic AF [3-4]. Traditionally, atrial pacing is performed in right atrial appendage (RAA). Recent research, however, indicates that atrial septal (AS) pacing produces better outcomes than the traditional RAA pacing [5-9]. The underlying mechanisms for this difference remained unclear.

One plausible explanation for the superiority of AS pacing over RAA pacing is that the two different regions have distinct electrophysiological properties. The heterogeneity of electrophysiology in the heart has long been recognized as a critical determinant of normal cardiac function and abnormally enhanced spatial dispersion of repolarization however plays a significant role in arrhythmogenesis [1, 2, 10-13]. Regional differences in repolarization and the underlying ionic currents between left and right atria [14], between the crista terminalis and pectinate muscles [15], and even within the right atrium [11], have been well documented and these differences are believed to contribute to the occurrence of AF [1, 2, 10-13]. Action potential variations between the right and left atrial roofs [14] or between the crista terminalis and pectinate muscles [15] in rabbit seem to involve in differences of transient outward K^+ current (I_{to}). The spatial differences of the ionic currents have been reported from canine atrial myocytes in detail, with corresponding differences in action potentials [11]. Recent studies have shown that regional heterogeneity of the ultrarapid delayed rectifier K^+ current (I_{Kur}) exist within the atria and I_{Kur} /I_{to} blockade reduces repolarization dispersion in right atrium [16, 17]. To date, no data have been available concerning the heterogeneity of action potential waveform and underlying ionic mechanisms between RAA and AS. Such information would be highly relevant to susceptibility to AF and to the treatment of AF [18, 19].

The present study was designed to explore whether there indeed exist regional differences of electrical activities between RAA and AS, using whole-cell current clamp and whole-cell voltage-clamp techniques. The object was to obtain data that can be used to explain why RAA and AS pacing produces different efficacies in AF management.

Materials and Methods

Patients

The study included 16 rheumatic heart disease (RHD) patients undergoing open-heart surgery from May 2005 to Nov 2007. The aims of these surgeries were mitral valve replacements. All patients were in normal sinus rhythm at the time of surgery, with no documented history of previous atrial fibrillation. The age of patients ranged from 37 to 70 years, averaging 52.1±2.6 years. Nine patients were female and seven patients were male. The investigations were approved by the Ethical Committee of the Harbin Medical University and performed in accordance with the principles outlined in the Declaration of Helsinki. Specimens of RAA were obtained early during the surgical procedure and before the institution of cardiopulmonary bypass. Tissues of AS were obtained after the hearts asystole by retro-perfuse cardioplegia solution through aorta. The characteristics of RHD patients are given in Table 1.

Cell isolation

Immediately after surgical excision, the specimens were placed in KB solution gassed with carbogen (5% CO_2, 95% O_2) at 4°C and quickly transported to laboratory within 15 min. We used a modified isolation procedure based on the technique described previously [12].

Myocardial specimens were cut into chunks and washed three times in oxygenated Ca^{2+} free Tyrode's solution at 37°C. And then the tissues were incubated in 10 mL Ca^{2+} free Tyrode's solution containing collagenase (0.25 mg/mL, type α, Sigma) and BSA (0.25 mg/mL) for 40 min at 37°C, the solution was always gassed with carbogen. Afterwards, tissues were transferred to fresh 10 mL Ca^{2+} free Tyrode's solution containing collagenase (0.13 mg/mL, type α). The incubation was finished as soon as microscopic examination revealed a satisfactory number of intact cardiomyocytes. Cells were then separated by centrifugation and resuspended in KB solution and kept at 4°C at least 1 h before they were used. Finally, the $CaCl_2$ concentration was increased again by 200 μM every 10 min to a final concentration of 1.8 mM.

Electrophysiological Recordings

Only rod-shaped myocytes with clear cross-striation were used. A small aliquot of the solution containing the isolated cells was placed in a 1-mL chamber mounted on the stage of an inverted microscope. The cells were allowed to adhere to the bottom of the chamber and then were continuously superfused with Tyrode's solution initially.

The whole-cell patch-clamp techniques were used to record ionic currents in the voltage-clamp mode using an Axopatch 200B amplifier (Axon Instruments), and action potentials (APs) were recorded in current-clamp mode. Borosilicate glass electrodes were connected to a headstage (CV 203 BU, Axon Instruments). When filled with pipette solution the electrodes had tip resistances from 2 to 4 MΩ. The potential of the pipette was zeroed before contacting the cell membrane in the bath solution. Voltage command pulses were

Table 1. Clinical characteristics of patients with RHD at the time of cardiac surgery. MVS, mitral valve stenosis; AVS, aortic valve stenosis.

Patient No.	Age (yr)	Gender	Diagnosis	Rhythm (beats/min)
1	65	Female	MVS	96
2	53	Female	MVS	67
3	37	Female	MVS, AVS	98
4	42	Female	MVS, AVS	64
5	52	Male	MVS, AVS	93
6	43	Male	MVS, AVS	68
7	51	Male	MVS, AVS	70
8	63	Female	MVS	69
9	70	Male	MVS	86
10	55	Female	MVS	94
11	46	Female	MVS	95
12	48	Female	MVS, AVS	84
13	61	Male	MVS, AVS	76
14	45	Male	MVS	93
15	60	Male	MVS	87
16	42	Female	MVS	79
Mean±SEM	52.1 ± 2.6	Female 56%; male 44%		82.4 ± 3.2

generated by a 12-bit digital-to-analog converter controlled by pClamp 9.0 software (Axon Instruments). Recordings were low pass-filtered at 1 kHz. Data were stored on the hard disk of an IBM-compatible computer. Junction potentials between bath and pipette solution averaged ≤10 mV and were corrected for APs only. Three minutes after seal formation, the membrane was ruptured by gentle suction to establish the whole-cell configuration. The capacitance and series resistance were compensated and all ionic currents data were expressed as current density (pA/pF) by normalizing the current to its capacitance for each cell. Cells with significant leak currents (seal resistance <1GΩ) were rejected.

APs, calcium current and all potassium currents except for I_{Kur} were recorded at 34-35°C with the use of a Peltier-effect device (N.B.Datyner). I_{Kur} and sodium current (I_{Na}) were studied at 19-20°C. Action potentials were recorded at a frequency of 0.1 Hz.

Solutions

The KB solution contained (in mM) glutamic acid 70, taurine 15, KCl 30, KH_2PO_4 10, HEPES 10, $MgCl_2$ 0.5, glucose 10, EGTA 0.5 at pH 7.4 adjusted by KOH. The standard Tyrode's solution contained (in mM) NaCl 136, KCl 5.4, $CaCl_2$ 1.8, $MgCl_2$ 1.0, NaH_2PO_4 0.33, HEPES 10, glucose 10; pH adjusted to 7.4 with NaOH. This solution was used as extracellular solution for action potential studies and was modified as indicated below when specific currents were studied. The pipette solution for action potential and potassium currents recordings contained (in mM) KCl 20, K-aspartate 110, $MgCl_2$ 1.0, HEPES 5, EGTA 10, Na_2ATP 5; pH adjusted to 7.2 with KOH. In order to measure selectively K^+ currents, I_{Na} was inactivated by using a holding potential (HP) of -40 mV or by adding tetrodotoxin (TTX, 30 μM, Sigma) in extracellular solution. Interference with calcium currents was omitted by the use of $CdCl_2$ (0.2 mM, Sigma) in the extracellular solution. For I_{to} recording, 4-Aminopyridine (4-AP, 50 μM) was added in extracellular solution to block I_{Kur}.

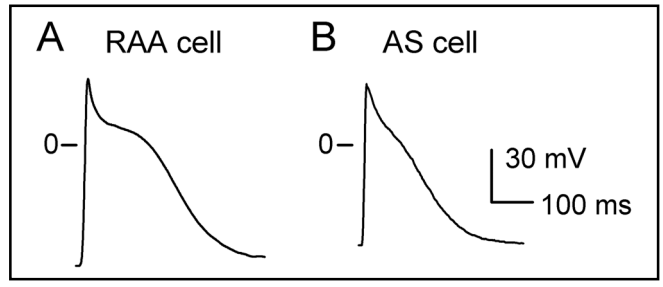

Fig. 1. Representative action potentials (APs) recorded in a RAA cell (A) and an AS cell (B) from a RHD patient.

The external solution for recordings of I_{Na} contained (in mM) CsCl 120, NaCl 25, HEPES 5, $MgCl_2$ 1.0, $CaCl_2$ 1.0, Glucose 10; pH adjusted to 7.4 with CsOH. The internal solution for I_{Na} recording contained (in mM) CsCl 20, CsF 110, NaCl 5, HEPES 5, EGTA 10, MgATP 5; pH adjusted to 7.2 with CsOH. The extracellular solution for L-type Ca^{2+} current (I_{CaL}) recording contained (in mM) 136 choline Cl, 5.4 CsCl, 1.0 $MgCl_2$, 2.0 $CaCl_2$, 5 HEPES, 10 glucose; pH adjusted to 7.4 with CsOH. The internal solution for I_{CaL} recording contained (in mM) 20 CsCl, 110 Aspartate acid, 110 CsOH, 5 HEPES, 1.0 $MgCl_2$, 10 EGTA, 5 MgATP; pH adjusted to 7.2 with CsOH.

Data Analysis

Group data are presented as mean ± SEM, and *n* indicates the number of cells from at least eight individual patients. Nonlinear and linear curve fittings were performed with the Clampfit routine in pCLAMP. Statistical comparisons among groups were performed by ANOVA and *t*-test. A two-tailed value of $P<0.05$ was taken to indicate statistical significance.

Region	*n*	RP (mV)	OS (mV)	APA (mV)	V_{max} (mV/ms)	APD_{50} (ms)	APD_{90} (ms)
RAA	16(8)	-63.0±0.8	40.2±1.1	103.2±1.4	168±4	189±29	345±34
AS	16(8)	-57.5±0.9**	37.3±0.9	94.7±1.4**	236±10**	118±19	246±23*

Table 2. Action potential characteristics of RAA and AS cells from patients with RHD. RP, resting potential; OS, overshoot; APA, amplitude of action potential; V_{max}, maximum upstroke velocity (dV/dt) of phase 0 of action potential; APD_{50} and APD_{90}, action potential duration at 50% and 90% of repolarization, respectively. *n* indicates the number of atrial myocytes, and the number in bracket indicates the number of patients. *P<0.05, **P<0.01 versus RAA group.

Results

The cell membrane capacitance determined in 80 RAA myocytes was 65.9±0.7 pF, and the capacitance determined in 78 AS myocytes was 100.2±0.4 pF (P<0.01).

Comparison of action potentials (APs) between RAA and AS cells

Figure 1 shows representative APs recorded from RAA (panel A) and AS (panel B) myocytes. We identified several important differences of APs between RAA and AS cells. First, the APs of RAA cells demonstrated prominent plateau phase whereas those in AS cells were triangular. This difference was also reflected by much longer AP duration (APD) in RAA than that in AS cells (RAA/AS ≈1.04, P<0.01). Second, resting membrane potential was significantly different, with ~6 mV more negative in RAA than that in AS cells (P<0.01). And third, AP amplitude was approximately 9 mV greater in RAA than that in AS cells (P<0.01). Correspondingly, the maximum upstroke velocity (V_{max}) of the rising phase of AP was also greater in AS cells (236±10 mV/ms, P<0.01) than that in RAA cells (168±4 mV/ms). Comparison of AP characteristics between RAA and AS cells is summarized in Table 2.

Comparison of sodium current (I_{Na}) between RAA and AS cells

Figure 2 shows typical examples of I_{Na} traces recorded from RAA and AS cells, respectively. I_{Na} was elicited, from an HP of -80 mV, by a series of 100-ms depolarizing test potentials (TP) from –60 mV to +40 mV with 10-mV increments. Detailed analyses revealed some significant differences of I_{Na} between RAA and AS cells. First, I_{Na} density was overall smaller in RAA cells relative to that in AS cells (P<0.01), but the statistically significant differences were limited to potentials negative to -10 mV (Fig. 2B); at the plateau range of voltages (between -10 mV and +10 mV), there was no significant difference of I_{Na} density between RAA and AS cells.

Second, the time-dependent properties of I_{Na} in RAA and AS cells were different. The kinetics of I_{Na} were analyzed by bi-exponential fitting to the descending phase of the current traces for activation and the rising phase for inactivation, and the results are displayed in Figure 2C. The time constants for activation (τ_{act}) and inactivation (τ_{inact}) derived from the fitting were averaged in Fig. 2D and it is clear that both activation and inactivation processes were faster in RAA cells, compared with AS cells. For instance, the τ_{act} at -30 mV where I_{Na} peaked was 0.40±0.02 ms in RAA cells and 0.61±0.04 ms in AS cells (P<0.01). Similarly, the τ_{inact} was 1.12±0.08 ms for RAA and 1.94±0.15 ms for AS (P<0.01).

And finally, the voltage-dependent properties of I_{Na} were different between RAA and AS cells (Fig. 3). Currents for activation were determined using a 50-ms prepulse of –100 mV to 100-ms test pulses between –100 and 0 mV from an HP of 0 mV. To evaluate the voltage dependence of activation, chord conductance was calculated using the equation: $g=I/(V_e-V_t)$, where g represents the conductance, I is the current amplitude measured at a test potential V_t, and V_e the equilibrium potential of Na^+ channels (+40 mV) calculated using the Nernst equation based on our experimental conditions. Then the g values at various potentials were normalized to the maximum g value at 0 mV and plotted against V_t to construct an activation curve. The relationship between g/g_{max} and membrane potential was fit by the Boltzmann function with $V_{1/2}$ values –42.8±2.0 mV in RAA (n=16)

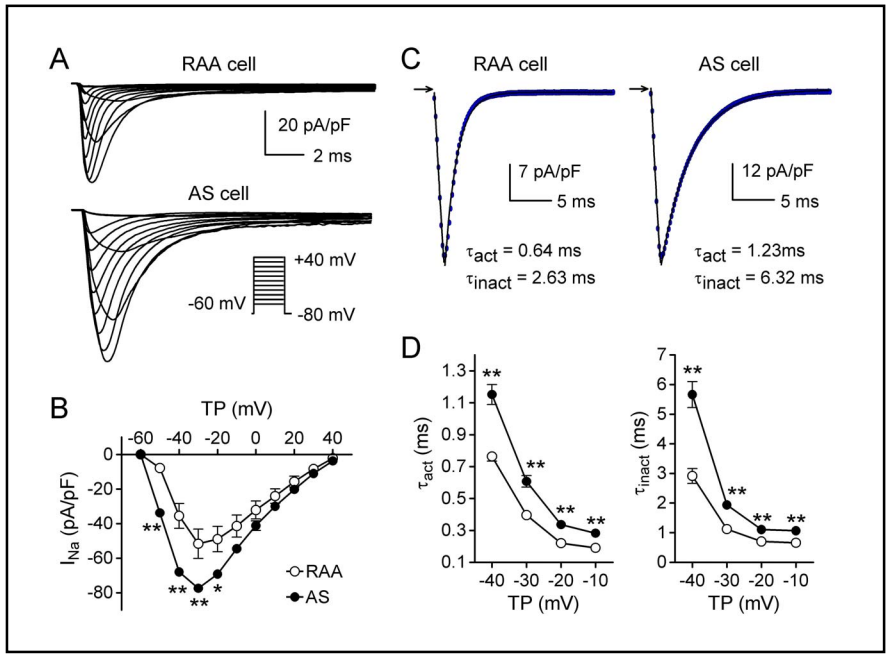

Fig. 2. Comparison of I_{Na} density and kinetics between RAA and AS cells of RHD patients. (A) I_{Na} traces from a RAA and an AS cell, respectively. (B) I_{Na} density-voltage relationships in RAA (n=16) and AS cells (n=16). (C) I_{Na} traces elicited by a 100-ms voltage step to –40 mV from –80 mV in a RAA (left panel) and an AS (right panel) cell. The raw data (points) were fitted by bi-exponential function (solid lines) and the descending phase represents the activation and the ascending phase the inactivation time courses. The arrows indicate the zero current level. (D) Voltage dependence of activation (left panel) and inactivation (right panel) time constants of I_{Na} in RAA (n=16) and AS cells (n=15). *P<0.05 or **P<0.01 versus RAA group.

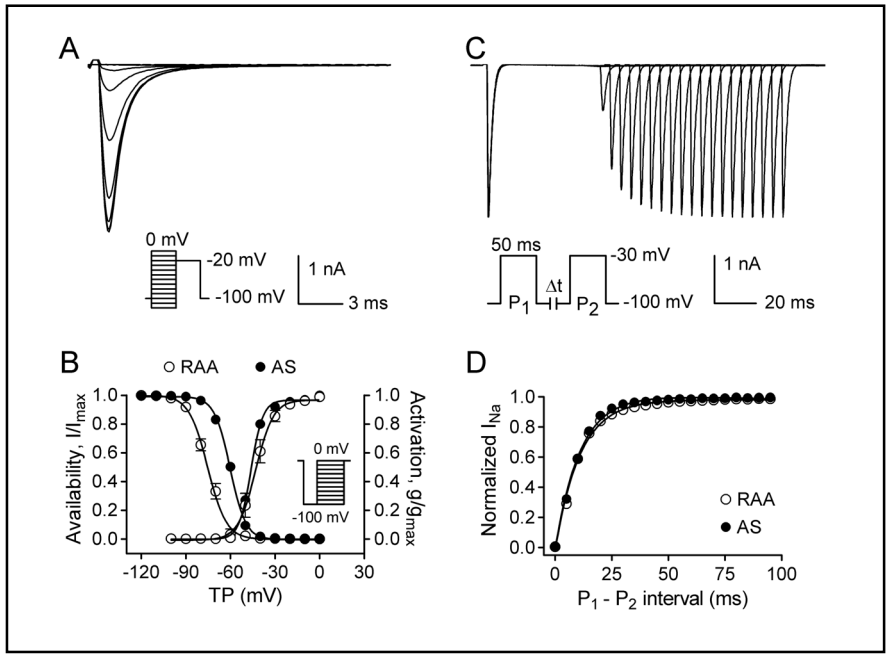

Fig. 3. Comparison of voltage-dependent properties of I_{Na} between RAA and AS cells of RHD patients. (A) Representative recordings and protocol used to assess inactivation (availability, I/I_{max}) in a RAA cell. (B) Voltage dependence of activation (g/g_{max}) and inactivation. I/I_{max} and g/g_{max} were fitted by Boltzmann distribution: $y=1/\{1+\exp[(V-V_{1/2})/S]\}$, where V is membrane potential, $V_{1/2}$ is the voltage for half-maximum current, and S is a slope factor. (C) Superimposed recordings of I_{Na} recovery from inactivation obtained in a RAA cell. P_1 and P_2 identical pulses delivered at varying P_1 and P_2 interval (Δt). (D) P_2 current normalized by P_1 current and plotted versus P_1-P_2 interval. Recovery curves were fitted with a mono-exponential function of the form I=A $\exp(-t/\tau)$.

and –46.2±0.8 mV in AS (n=16) myocytes. Accordingly, the slope factors were 3.0±0.4 and 3.4±0.2 mV, respectively. The voltage-dependent inactivation properties were assessed using a two-step protocol: the membrane was first stepped to potentials between –120 and 0 mV to condition I_{Na} and then pulsed to a test potential of–20 mV to record I_{Na}. I_{Na} inactivation curves were constructed by plotting relative availability of I_{Na} (I/I_{max}: I_{Na} amplitude at various conditioning potentials divided by the maximum I_{Na} amplitude at -120 mV) as a function of the conditioning potential. The voltage dependence of inactivation was fit by the Boltzmann function to determine the voltage for half availability of I_{Na} ($V_{1/2}$) and the slope factor. The $V_{1/2}$ values were around 14 mV more negative in RAA myocytes (–74.7±1.6 mV, n=16) than those in AS myocytes (–60.1±0.5 mV, n=15, P<0.01). The slope factors were 6.3±0.2 and 5.2±0.3 mV for RAA and AS cells (P<0.01), respectively.

The time dependence of I_{Na} recovery from inactivation was studied using a paired-pulse protocol

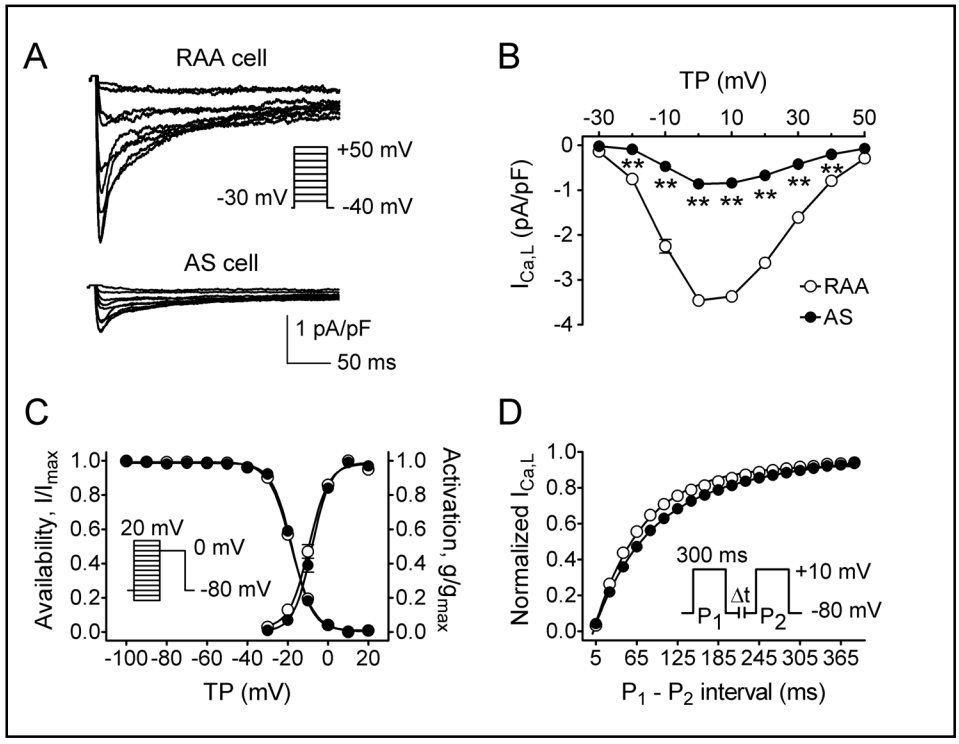

Fig. 4. Comparison of I_{CaL} density and voltage-dependent properties between RAA and AS cells of RHD patients. (A) Typical recordings of I_{CaL} from a RAA cell and an AS cell, respectively. (B) I_{CaL} density-voltage relations. (C) I_{CaL} activation and inactivation curves. (D) Reactivation time course of I_{CaL}. 12 cells for each region, *P<0.05 or **P<0.01 versus RAA group.

illustrated in Figure 3C: identical clamp pulses (P_1, P_2) were delivered from an HP of –100 mV to a step potential of -30 mV with a variable interpulse interval (5 ms increment, P_1-P_2) at 0.2 Hz. The current during P_2 (I_2) relative to the current during P_1 (I_1) was plotted as a function of the P_1-P_2 reactivation interval (Fig. 3D). The reactivation curves were fitted by mono-exponential function to determine the reactivation time course. There was no significant difference of recovery time constants between RAA (11.2±1.0 ms, n=16) and AS myocytes (10.8±0.4 ms, n=16).

Comparison of L-type Ca^{2+} current (I_{CaL}) between RAA and AS cells

I_{CaL} was evoked by depolarizing pulses ranging from -30 mV to +50 mV from an HP of -40 mV (Fig. 4). Striking differences of I_{CaL} was found between RAA and AS cells; I_{CaL} density in RAA cells was nearly 4-fold larger than that in AS cells at the plateau voltage range (from -10 mV to +20 mV). For instance, at 0 mV, I_{CaL} averaged -3.46±0.12 pA/pF in RAA cells (n=12) and -0.86±0.03 pA/pF in AS cells (n=12, P<0.01).

Figure 4C shows the voltage-dependence of I_{CaL} activation and inactivation. The activation of I_{CaL} was determined from the *I-V* relation in figure 4B, using the equation of $g=I/(V_e-V_t)$, where V_e represents the equilibrium potential of Ca^{2+} channels. The relationship between g/g_{max} and membrane potential was fit by the Boltzmann function with $V_{1/2}$ –9.1±1.0 mV in RAA cells and –8.0±0.8 mV in AS cells (n=12 in both regions). Accordingly, the slope factors were 4.4±0.1 and 4.2±0.2 mV, respectively. The voltage-dependence of I_{CaL} inactivation was recorded using a two-step protocol (see *inset*): the membrane was first stepped to 300 ms potentials between –100 and +20 mV to condition I_{CaL} and then 0 mV to test the extent of inactivation. $I_{Ca,L}$ inactivation curves were obtained by plotting relative availability (I/I_{max}) of I_{CaL} as a function of the conditioning potential. The voltage dependence of inactivation could be fit by the Boltzmann function with $V_{1/2}$ –18.4 ± 0.8 mV in RAA cells and –17.9±0.6 mV in AS cells (n=12 in both region). Accordingly, the slope factors were 5.7±0.6 and 4.8±0.4 mV, respectively. No apparent difference in the voltage-dependent activation and inactivation properties was observed.

The time dependence of I_{CaL} recovery from inactivation was studied using a paired-pulse protocol (Fig. 4D): identical clamp pulses (P_1, P_2) were imposed from an HP of –80 mV to a step potential of +10 mV with a variable interpulse interval (20ms increment) at 0.2 Hz. The reactivation curves were fitted by a bi-exponential function of $y=A_1\exp(-t/\tau_1)+A_2\exp(-t/\tau_2)+y0$. τ_1 averaged 55±3 ms in RAA and 72±5 ms in AS cells (n=12/region, P<0.05); τ_2 averaged 335±22 ms in RAA and 375±48 ms in AS cells.

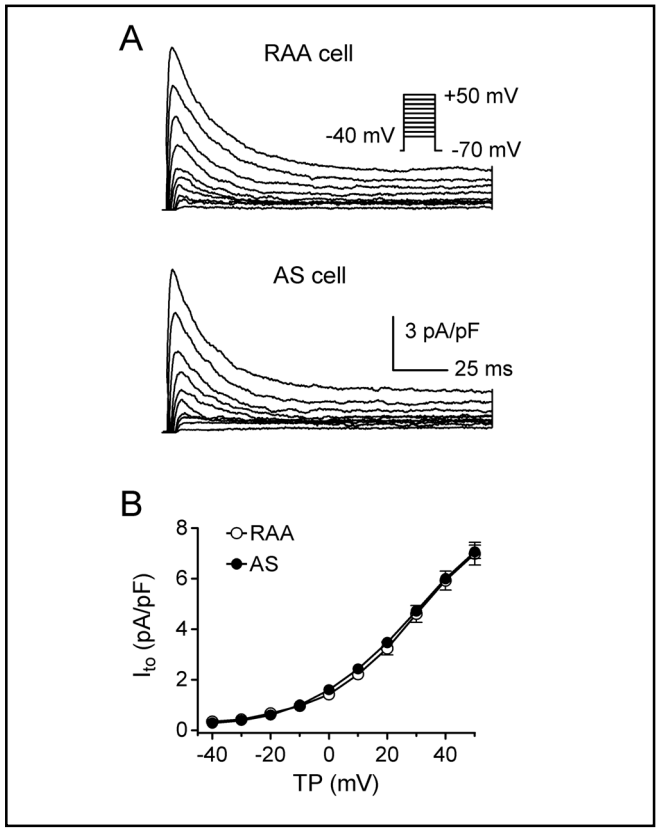

Fig. 5. Comparison of I_{to} density between RAA and AS cells of RHD patients. (A) Typical recordings of I_{to} from a RAA cell and an AS cell, respectively. (B) I_{to} density-voltage relations for each region (n=16 in RAA and 15 in AS).

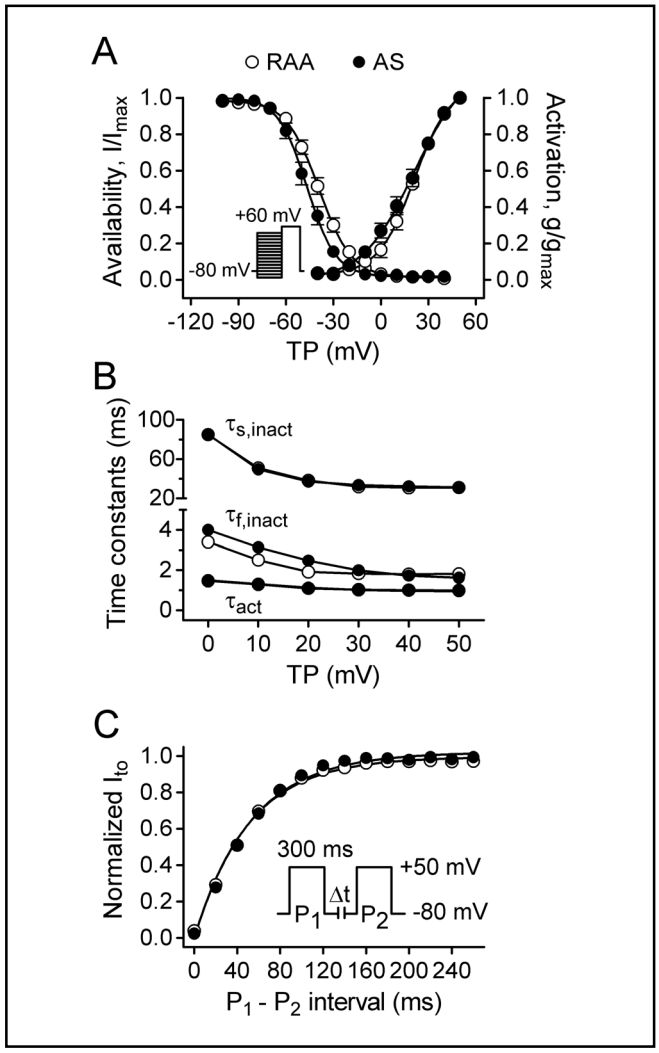

Fig. 6. Comparison of steady-state voltage-dependent and time-dependent properties of I_{to} between RAA and AS cells of RHD patients. (A) I_{to} activation (n=14 in each group) and inactivation (n=16 in RAA and 15 in AS) curves. (B) Activation and inactivation time constants of I_{to} (14 cells/region). (C) Reactivation time course of I_{to} (n=16 in RAA and 14 in AS).

Comparison of transient outward K^+ current (I_{to}) between RAA and AS cells

I_{to} was studied with 150-ms depolarizing pulses between –40 and +50 mV from an HP of –70 mV at 0.5 Hz. The amplitude of I_{to} was measured as the difference between the peak outward current and the current at the end of the clamp pulse. Figure 5 shows typical recordings of I_{to} in the cells from RAA and AS. There were no significant differences in I_{to} density between RAA and AS cells; mean current densities at +50 mV averaged 7.0±0.5, 7.1±0.3 pA/pF in RAA (n=16) and AS (n=15) cells, respectively (Fig. 5B).

The voltage-dependence of I_{to} activation was determined from the I-V relation. The equation of form $g=I/(V_e-V_t)$ was used, where V_e represents the equilibrium potential of K^+ channels. The data points were fitted by the Boltzmann function to obtain half-activation voltage ($V_{1/2}$) and slope factor (Fig. 6). No significant regional differences in the voltage dependence of I_{to} activation were observed. $V_{1/2}$ and slope factors were 18.4±2.4 and 13.7±2.4 mV in RAA (n=14), and 15.5±3.3 and 16.0±2.1 mV in AS (n=14), respectively.

Voltage-dependent inactivation was studied with 400-ms pre-pulses between –100 and +40 mV from an HP of –80 mV, followed by a 300-ms test pulse to +60 mV. The amplitudes of current were normalized and plotted against the voltage of the conditioning pulses. The half-inactivation voltage and slope factor averaged –39.7±1.7 and 9.4±0.8 mV in RAA (n=16), and -47.6±2.1 and 7.5±0.5 mV in AS (n=15), respectively.

I_{to} activation was well fitted by a mono-exponential function and the inactivation kinetics was fitted by a bi-

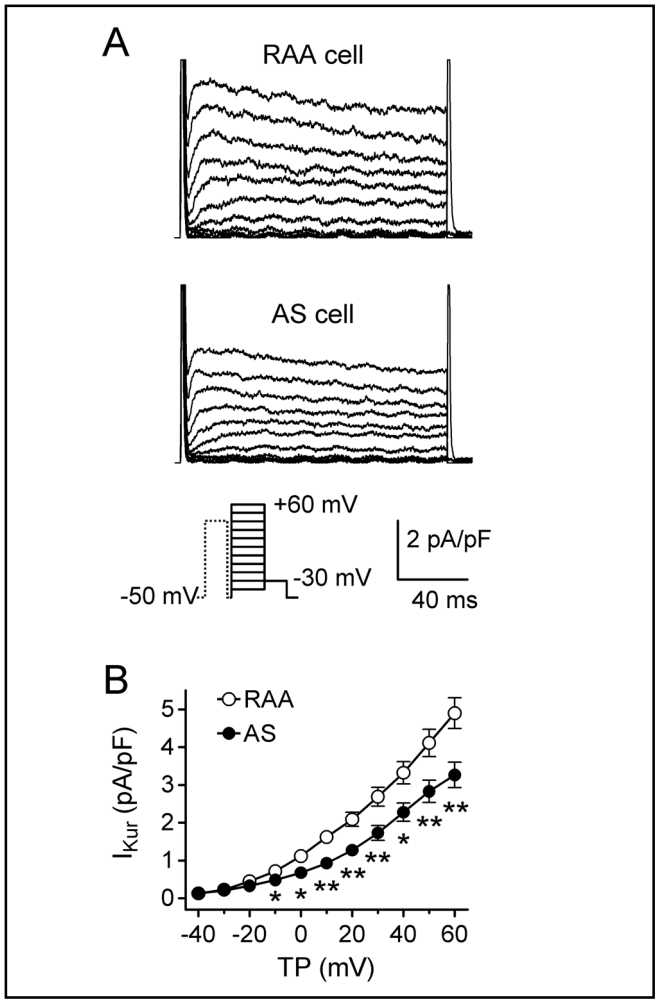

Fig. 7. Comparison of I_{Kur} density between RAA and AS cells of RHD patients. (A) Typical recordings of I_{Kur} from a RAA cell and AS cell, respectively. (B) I_{Kur} density-voltage relations for RAA (n=18) and AS (n=16) cells. *P<0.05, **P<0.01 versus RAA group.

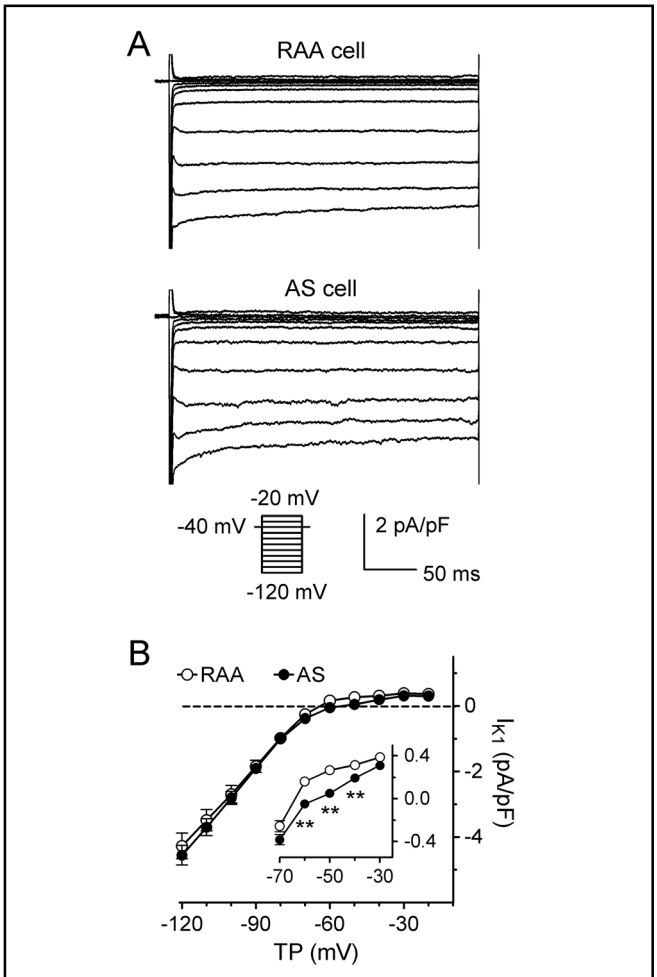

Fig. 8. Comparison of I_{K1} density between RAA and AS cells of RHD patients. (A) Typical recordings of I_{K1} from a RAA cell and an AS cell, respectively. (B) I_{K1} density-voltage relations for RAA and AS cells (n=16 in each group, *P< 0.01). The *inset* shows the outward I_{K1} current at potentials between -70 mV and -30 mV.

exponential function. The results indicate no significant interregional differences between RAA and AS (Fig. 6B). Recovery from inactivation of I_{to} was assessed with the use of paired pulses (P_1, P_2) of 300-ms duration to +50 mV from an HP of –80 mV with varying interpulse intervals (20ms increment) at 0.2 Hz. The amplitude of I_{to} elicited by P_2 was normalized to I_{to} elicited by P_1 and was plotted versus the interpulse intervals (Fig. 6C). Data were fitted by mono-exponential function, and no significant interregional differences were found. The recovery time constants averaged 54.7±4.2 ms in RAA (n=16) and 54.4±3.9 ms in AS cells (n=14).

Comparison of ultrarapid delayed rectifier K^+ current (I_{Kur}) between RAA and AS cells

To record I_{Kur}, a 100-ms prepulse of +40 mV was applied to inactivate I_{to}, followed by 150-ms test pulses between –40 and +60 mV from –50 mV after a 10-ms interval at 0.5 Hz. I_{Kur} was measured from zero current to the steady-state level at the end of depolarization step. I_{Kur} density was significantly larger at potentials from -10 mV to +60 mV in RAA cells than that in AS cells (Fig. 7). For instance, at +60 mV, I_{Kur} density averaged 4.9±0.4 pA/pF in RAA cells and 3.3±0.3 pA/pF in AS cells (P<0.01).

Comparison of inward rectifier K^+ current (I_{K1}) between RAA and AS cells

I_{K1} was elicited by 300-ms pulses from an HP of –40 mV to voltages ranging from –120 mV to -20 mV at 0.2 Hz (Fig. 8). No significant regional differences in I_{K1} density between RAA and AS were observed at potentials from –120 to –70 mV; I_{K1} density at –120 mV averaged -4.3±0.4 and –4.6±0.3 pA/pF in RAA (n=16) and AS (n=16), respectively. However, significantly greater outward I_{K1} at voltages of -60 mV, -50 mV and -40 mV was seen in RAA than that in AS cells.

Discussion

In this study, we compared in detail the electrical activities at the cellular level (action potentials) and ionic level (ion currents) between right atrial appendage (RAA) and atrial septum (AS) of the same heart. The major finding of this study is that RAA and AS of patients with RHD possess distinct electrophysiological properties, which are well reflected by their different morphologies and durations of action potentials (APs), and by their different biophysical properties and densities of ionic currents. These differences provided a rational explanation for the different efficacies in treating AF by atrial pacing in RAA and AS regions.

The main differences in APs between RAA and AS cells are resting membrane potential (RMP) and AP duration (APD); RAA cells generally have more negative RMP and longer APD. Consistent with the more polarized membrane potential in RAA cells, I_{K1} current densities at potentials between -60 mV and -40 mV where outward I_{K1} was seen were significantly larger in these cells relative to those in AS cells. APD is determined by the balance between inward and outward currents operating during the period of excitation. In this study, we found smaller I_{Na} and greater I_{Kur} in RAA compared with AS cells; based on these data one would expect to see shorter APD in RAA than that in AS cells. However, I_{CaL} is remarkably larger (approximately 4 folds) in RAA than in AS cells and this APD-prolonging force overweighed the APD-shortening factors (smaller I_{Na} and greater I_{Kur}), conferring longer APD in RAA cells. We consistently observed greater V_{max} and sodium channel availability in AS cells than that in RAA cells (table 2 and Figure 3), despite that the resting potential is more negative in RAA (-63.0 mV) than in AS (-57.5 mV). This seemingly "contradictory" observation could be explained by the fact that at -63.6 mV, the availability in RAA is 0.133, which is substantially smaller than the availability in AS cells at -57.2 mV (0.352).

Our study elucidated the electrophysiological basis at the cellular and ionic levels for the clinically observed differences of effectiveness of RAA and AS pacing in preventing recurrence of AF. It is known that one of the most important characteristics of electrical remodeling in AF is impaired intracellular Ca^{2+} handling leading to Ca^{2+} overload in atrial myocytes. During an excitation, Ca^{2+} enters into the cytosol with repeated rapid pacing and more Ca^{2+} influx is expected. The greater I_{CaL} in RAA cells is deemed to allow for a greater Ca^{2+} influx. Moreover, APD in RAA is much longer than that in AS cells, which should allow for more Ca^{2+} entry into the cell during an AP. Thus, an intracellular Ca^{2+} overload may more readily happen in RAA cells. In contrast, I_{Na} density is larger in AS cells, which would allow for faster conduction in these cells compared with RAA cells. It should be noted that these points of views are highly speculative and detailed future studies are needed to clarify these issues. The present work lays the groundwork for the future studies.

One important limitation of this study is the lack of healthy hearts as a control. The reason for that is on one hand, we have had restricted cases of explanted hearts for the study, and on the other hand, we figured that the atrial tissues from patients with rheumatic heart disease (RHD) might be of better choice for the particular purpose of our study. The objective of the present study was to decipher the cellular and ionic mechanisms underlying the different efficacies for preventing the recurrent atrial fibrillation (AF) between RAA pacing and AS pacing. It is obviously more rational to conduct our study with atrial samples that are more closely relevant to AF. And it is well known that patients with RHD are highly susceptible to AF induction; nearly one-quarter of RHD patients have AF [20-22]. Moreover, in our study the comparisons were made between RAA and AS in pairs from the same hearts and it is hard, if not impossible, to obtain such samples from healthy individuals.

Acknowledgements

This study was supported by the National Basic Research Program of China (973 Program, 2007CB512000/2007CB512006, to B. Yang; 2007CB516803, to Y. Lu), the Education Department Foundation of Heilongjiang Province of China (11511231), and the Health Department Plan of Heilongjiang Province of China (2006-324).

References

1 Waktare JE, Camm AJ: Atrial fibrillation begets trouble. Heart 1997;77:393–394.

2 Nattel S: Newer developments in the management of atrial fibrillation. Am Heart J 1995;30:1094–1106.

3 Yee R, Klein GJ, Krahn AC, Skanes AC: Selective site pacing: tools and training. Pacing Clin Electrophysiol 2004;27(6 Pt 2):894-896.

4 Gammage MD, Marsh AM: Randomized trials for selective site pacing: do we know where we are going? Pacing Clin Electrophysiol 2004;27(6 Pt 2):878-882.

5 Padeletti L, Porciani MC, Michelucci A, Colella A, Ticci P, Vena S, Costoli A, Ciapetti C, Pieragnoli P, Gensini GF: Interatrial septum pacing: a new approach to prevent recurrent atrial fibrillation. J Interv Card Electrophysiol 1999;3:35–43.

6 Padeletti L, Pieragnoli P, Ciapetti C, Colella A, Musilli N, Porciani MC, Ricci R, Pignalberi C, Santini M, Puglisi A, Azzolini P, Spampinato A, Martelli M, Capucci A, Boriani G, Botto G, Proclemer A: Randomized crossover comparison of right atrial appendage pacing versus interatrial septum pacing for prevention of paroxysmal atrial fibrillation in patients with sinus bradycardia. Am Heart J 2001;142(6):1047-1055.

7 Ogawa M, Kumagai K, Gondo N, Matsumoto N, Suyama K, Saku K: Novel electrophysiologic parameter of dispersion of atrial repolarization: comparison of different atrial pacing methods. J Cardiovasc Electrophysiol 2002;13:110–117.

8 Padeletti L, Michelucci A, Pieragnoli P, Colella A, Musilli N: Atrial septal pacing: a new approach to prevent atrial fibrillation. Pacing Clin Electrophysiol 2004;27:850–854.

9 de Voogt WG, van Mechelen R, van den Bos AA, Scheffer M, van Hemel NM, Levine PA: Electrical characteristics of low atrial septum pacing compared with right atrial appendage pacing. Europace 2005;7(1):60-66.

10 Spach MS, Dolber PC, Anderson PA: Multiple regional differences in cellular properties that regulate repolarization and contraction in the right atrium of adult and newborn dogs. Circ Res 1989;65:1594–1611.

11 Feng J, Yue L, Wang Z, Nattel S: Ionic mechanisms of regional action potential heterogeneity in the canine right atrium. Circ Res 1998;83:541–551.

12 Wang Z, Fermini B, Nattel S: Delayed rectifier outward current and repolarization in human atrial myocytes. Circ Res 1993;73:276–285.

13 Wang Z, Feng J, Nattel S: Idiopathic atrial fibrillation in dogs: underlying electrophysiologic determinants and mechanism of antiarrhythmic action of flecainide. J Am Coll Cardiol 1995;26:277–286.

14 Qi A, Yeung-Lai-Wah JA, Xiao J, Kerr CR: Regional differences in rabbit atrial repolarization: importance of transient outward current. Am J Physiol 1994;266:H643–H649.

15 Yamashita T, Nakajima T, Hazama H, Hamada E, Murakawa Y, Sawada K, Omata M: Regional differences in transient outward current density and inhomogeneities of repolarization in rabbit right atrium. Circulation 1995;92:3061–3069.

16 Burashnikov A, Mannava S, Antzelevitch C: Transmembrane action potential heterogeneity in the canine isolated arterially perfused right atrium: effect of I_{Kr} and I_{Kur}/I_{to} block. Am J Physiol Heart Circ Physiol 2004;286:H2393–H2400.

17 Wettwer E, Hála O, Christ T, Heubach JF, Dobrev D, Knaut M, Varró A, Ravens U: Role of I_{Kur} in controlling action potential shape and contractility in the human atrium: influence of chronic atrial fibrillation. Circulation 2004;110:2299–2306.

18 Fynn SP, Todd DM, Hobbs WJ, Armstrong KL, Garratt CJ: Role of dispersion of atrial refractoriness in the recurrence of clinical atrial fibrillation; a manifestation of atrial electrical remodelling in humans? Eur Heart J 2001;22:1822–1834.

19 Soylu M, Demir AD, Ozdemir O, Soylu O, Topaloðlu S, Kunt A, Sasmaz A, Korkmaz S, Taþdemir O: Increased dispersion of refractoriness in patients with atrial fibrillation in the early postoperative period after coronary artery bypass grafting. J Cardiovasc Electrophysiol 2003;14:28–31.

20 Diker E, Aydogdu S, Ozdemir M, Kural T, Polat K, Cehreli S, Erdogan A, Goksel S: Prevalence and predictors of atrial fibrillation in rheumatic valvular heart disease. Am J Cardiol 1996;77(1):96-98.

21 Vora A: Management of atrial fibrillation in rheumatic valvular heart disease. Curr Opin Cardiol 2006;21(1):47-50.

22 Kumar AS, Talwar S, Saxena A, Singh R, Velayoudam D: Results of mitral valve repair in rheumatic mitral regurgitation. Interact Cardiovasc Thorac Surg 2006;5(4):356-361.